Artificial Intelligence in Agriculture 2 (2019) 28–37

Contents lists available at ScienceDirect

Artificial Intelligence in Agriculture

journal homepage: http://www.keaipublishing.com/en/journals/artificial-intelligence-in-agriculture/

A computer vision system for defect discrimination and grading in tomatoes using machine learning and image processing

David Ireri [a], Eisa Belal [a,b], Cedric Okinda [a], Nelson Makange [a], Changying Ji [a,*]

[a] College of Engineering, Laboratory of Modern Facility Agriculture Technology and Equipment Engineering of Jiangsu Province, Nanjing Agricultural University, Jiangsu 210031, PR China
[b] Faculty of Agriculture, Department of Agricultural Engineering, University of Zalingei, Central Darfur State, R., Sudan

ARTICLE INFO

Article history:
Received 21 April 2019
Received in revised form 6 June 2019
Accepted 6 June 2019
Available online 17 June 2019

Keywords:
Grading
Calyx
Defected
Recognition models
Machine vision

ABSTRACT

With large-scale production and the need for high-quality tomatoes to meet consumer and market standards criteria, have led to the need for an inline, accurate, reliable grading system during the post-harvest process. This study introduced a tomato grading machine vision system based on RGB images. The proposed system performed calyx and stalk scar detection at an average accuracy of 0.9515 for both defected and healthy tomatoes by histogram thresholding based on the mean g-r value of these regions of interest. Defected regions were detected by an RBF-SVM classifier using the LAB color-space pixel values. The model achieved an overall accuracy of 0.989 upon validation. Four grading categories recognition models were developed based on color and texture features. The RBF-SVM outperformed all the explored models with the highest accuracy of 0.9709 for healthy and defected category. However, the grading accuracy decreased as the number of grading categories increased. A combination of color and texture features achieved the highest accuracy in all the grading categories in image features evaluation. This proposed system can be used as an inline tomato sorting tool to ensure that quality standards are adhered to and maintained.

1. Introduction

Tomato a nutritious and nourishment fruit is one of the top-grown agricultural produce in the world. According to (FAOSTAT, 2017), the global production of tomatoes was 170.8 million tons with China as the leading producer accounting for over 31% of the total production. With large-scale production, the post-harvest procedure is crucial since tomato is a delicate and a perishable fruit. Additionally, quality and food safety are decisive factors in tomato supply chain management to meet trade specifications and buyer's requirements (Esguerra et al., 2018). According to EU (2011) on the regulations for processed fruits and vegetables, the minimal requirements is that tomatoes must appear fresh, intact, free from deterioration, free of cracks, free from damage and must arrive at the destination in a satisfactory condition. Thus, identifying these traits assists in conforming to the accepted market standards.

Several chemical and physical parameters affect fruit quality and have been used to sort and grade tomatoes during post-harvesting such as size (large and small), shape (circular or oblong), defects and maturity or color (Arjenaki et al., 2013). These parameters have helped in identifying tomatoes with mechanical damage, disease, and insect damage, cracks, and pre-harvest deformation defects to achieve the required market standards (FAO, 2008). Furthermore, sorting governs effectiveness and efficiency on how the product will be marketed through the packing lines and quality standard. Thus, it is essential to have a sorting method which is robust, consistent, fast, effective, and non-destructive (Jarimopas and Jaisin, 2008).

The common sorting and grading technique is manual sorting. However, this technique suffers from several disadvantages, such as low precision, labor-intensive, and subjectivity (Karlsson, 2016). Gould (1975) introduced the mechanical tomato sorting machine as a solution to the shortcomings of manual sorting. However, this grading system was limited to only size and weight classification. Presently, with the emergence and developments in machine vision technology, it has become possible to overcome these limitations accurately and non-destructively based on machine vision detection systems (Chen et al., 2002).

Computer vision-based systems have already been applied in vast areas of food and agricultural-based industry in the sorting of apple (Moallem et al., 2017; Unay et al., 2011), strawberry (Liming and Yanchao, 2010), tomato (Arakeri, 2016; Clement et al., 2012), potatoes (Moallem et al., 2013), dates (Al Ohali, 2011; Lee et al., 2008), citrus (Blasco et al., 2007; López-García et al., 2010), mangos (Naik and Patel, 2014; Naik et al., 2015; Nandi et al., 2014), cucumbers (Clement et al., 2013) etc. Tomato sorting based on machine vision was reported as early as 1985 by Sarkar and Wolfe (1985), this study graded the tomatoes depending on size, color shape, and defected. However, this

* Corresponding author.
E-mail address: chyji@njau.edu.cn (C. Ji).

https://doi.org/10.1016/j.aiia.2019.06.001

system required the fruits to lie on their stem or blossom ends orientation during imaging for feature extraction. Clement et al. (2012) introduced a tomato classifier based on color, size, and weight. However, as earlier mentioned, fruit quality is also affected by defects. Defects detection based on color features was reported by Dhanabal and Samanta (2013) in the detection of Blossom End Rot (BER) and Rokunuzzaman and Jayasuriya (2013) in the detection of BER and cracks. Color features are considered as first-order spatial statistics that depend on individual pixel values. However, a defect has no spatial direction. Thus, relative regions of the defects should be taken into account (Arakeri, 2016; Moallem et al., 2017). To improve on tomato defect detection, Arakeri (2016) proposed the use of high-quality images and image texture features. However, the use of high-resolution images such as hyperspectral, and multispectral (Moltó et al., 2010; Polder and van der Heijden, 2010) imaging system have been reported to consume much computational time and high costs involved (Arakeri, 2016).

This study introduces a low-cost tomato grading system based on color images processing and machine learning technology. The proposed system extracted both LAB color features and gray level texture features and used them as feature variables to develop correlations to tomato redness color intensity and defect. LAB color space is often less affected by the variations of the camera sensor compared to RGB (Shafiee et al., 2014). Texture features are also referred to as second-order features (Moallem et al., 2017) because they capture the spatial dependence of gray values that contribute to the perception of texture by representing the properties of pixels in pairs. The main objective of this study was to develop a computer vision system that can be used to grade tomatoes. The specific objectives of this study were to develop an efficient image processing algorithm, to develop an efficient and accurate calyx detection algorithm and to develop different classifiers to grade tomatoes into different grading categories. This proposed system can be applied in real-time tomato post-harvesting procedures because its fast, cheap, accurate, and non-detective, thus improved reduced inspection time and quality sorting guarantee in tomato production and supply chain management.

2. Materials and methods

2.1. Experiment setup and data collection

Experiments were conducted between November 2018 and January 2019 at Nanjing Agricultural University, College of Engineering, Nanjing, Jiangsu Province, China. A total of 200 tomatoes with different degree of defects and red color intensity were manually selected at a local farm in Jiangpu, Nanjing, Jiangsu China. Cherry tomatoes and Heirloom tomatoes were used. The overview of the proposed system is given in Fig. 1.

The image acquisition system was composed of Hikvision Mini Camera (DS-2CD2D14WD/M4MM), mounted 1.0 m perpendicularly above an imaging stage, as shown in Fig. 2. The camera was connected via an Ethernet to an intel core i5-4500U CPU, 4 GHz, 16 GB physical memory (Intel, Santa Clara, CA, USA), Microsoft Windows 10 PC. Images of tomatoes (1280 × 720) at different orientations were acquired at 10 fps. For each tomato, ten images were selected for subsequent analysis.

2.2. Image processing and feature extraction algorithms

These algorithms aimed at developing a tomato grading system based on defects and color intensity, as shown in Fig. 1. Firstly, segmentation algorithms were applied to the captured image to remove the background. Secondly, performed calyx and stalk scar detection and

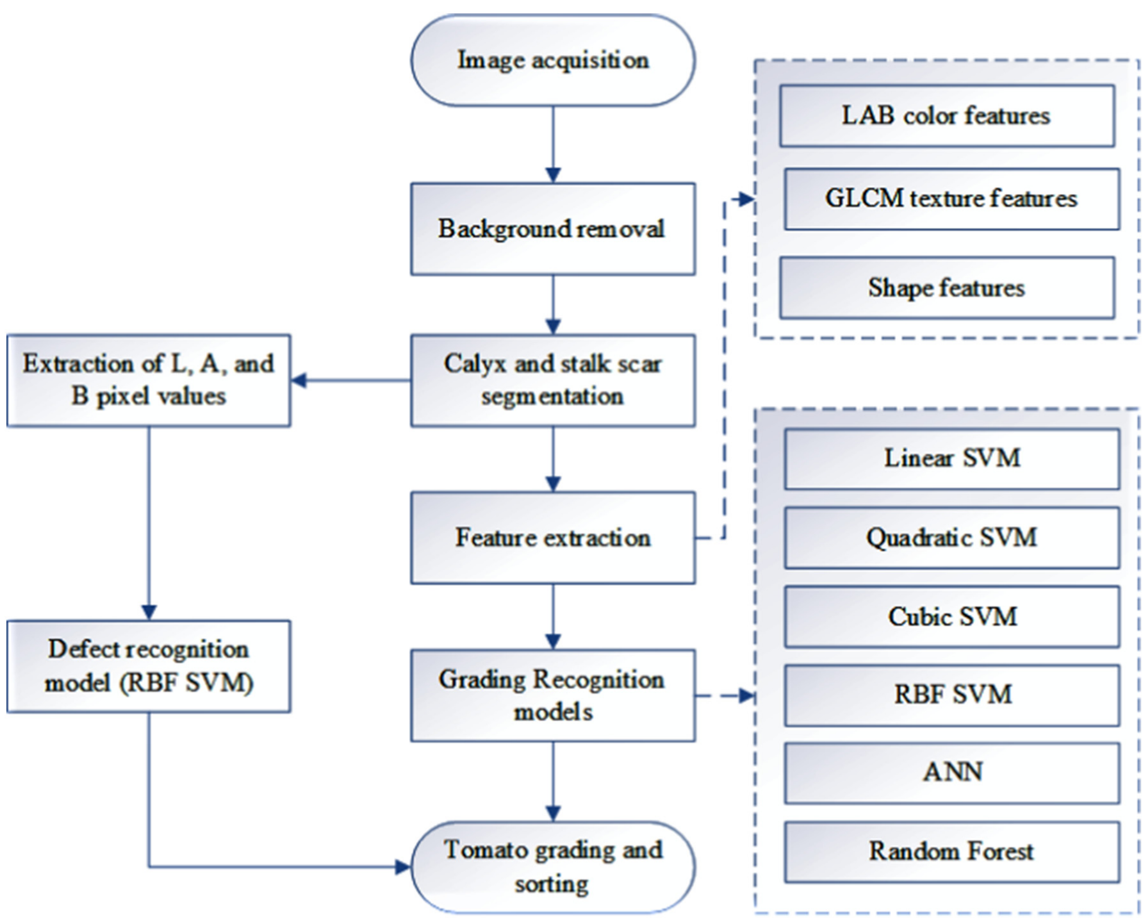

Fig. 1. The algorithmic flow of the proposed system.

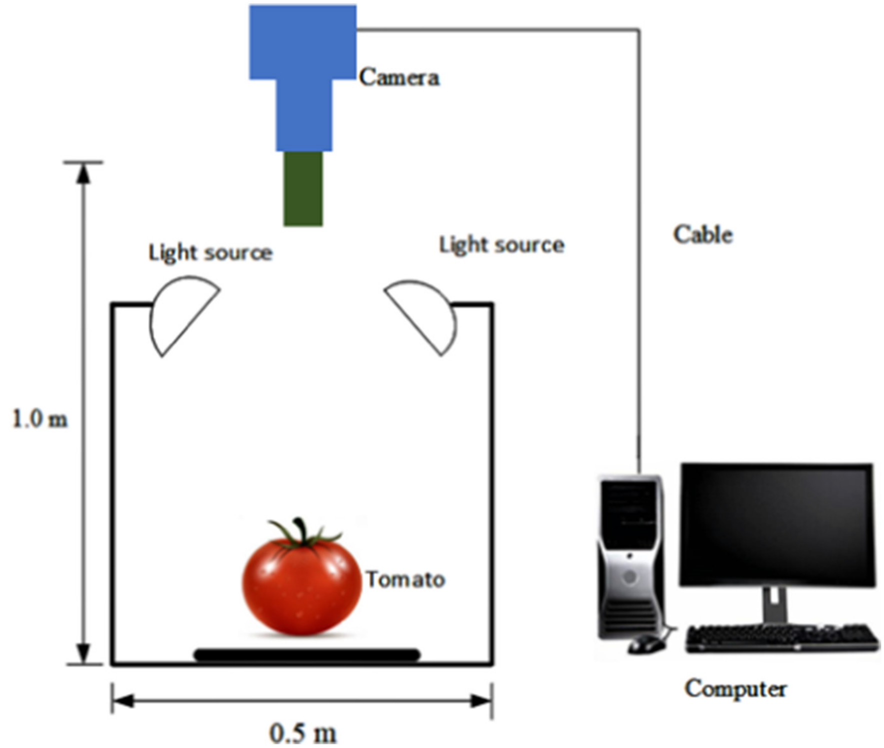

Fig. 2. Experiment setup and Image acquisition system.

defect segmentation. Thirdly extracted the color, texture, and shape features from all the images. Fourthly, developed classifiers based on support vector machines (SVM), artificial neural network (ANN), and random forest for comparative analysis of proposed tomato grading technique.

2.3. Image processing

2.3.1. Background removal

In this study, the image acquisition system was stationary. Thus, a simple image subtraction technique was used for background removal. Due to RGB images being sensitive to the ambient light conditions, the background was incompletely removed in some images. However, in the set-up condition, the background pixels had lower values than the foreground pixels. Hence, the background was entirely removed by a histogram thresholding technique, as shown in Fig. 3. The threshold was calculated by Eq. (1) (Moallem and Razmjooy, 2012)

$$\delta = \frac{1}{2}(\mu_{mxr} + \mu_m) \tag{1}$$

where, δ is the heuristic threshold value, μ_{mxr} is the gray level with the most repetitions in the image, and μ_m is the median of the gray level distribution of the image.

2.3.2. Calyx and stalk scar detection

The calyx and stalk scar (CS) are often very similar to a defect in terms of appearance, as shown in Fig. 4(a) and (d). Thus, it is necessary to segment them before classifying a tomato. In this study, the CS was detected based on the gray values of a tomato image along with the longitudinal directions of the tomato image. Fifty images with clear CS were selected for the development of the CS detection algorithm. Based on these experiments, it was established that the g-r values of

Fig. 3. Image background removal, (a) original color image, (b) original image without the background.

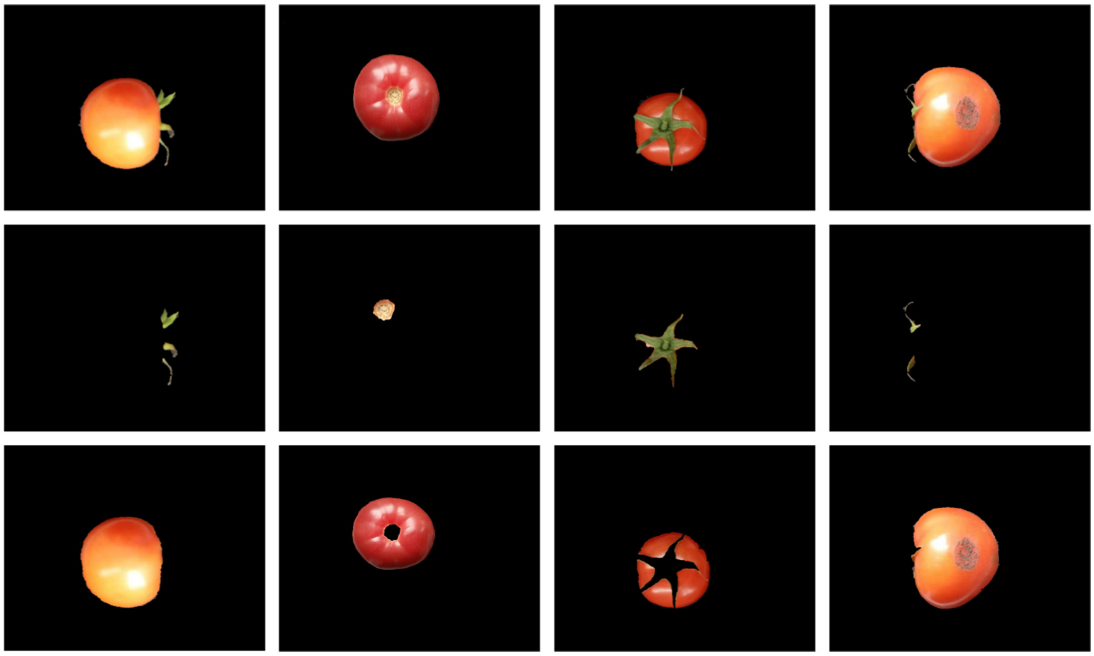

Fig. 4. Calyx and stalk scar detection and segmentation, (a) original RGB image (b) Detected calyx and stalk scar, and (c) Calyx and stalk scar segmentation.

the CS were greater than that of the fruit. Thus, they were segmented by a histogram threshold (Eq. (1)) based on the average value of the g-r value of the CS regions of the selected images.

2.3.3. Defect detection

Tomato is a very succulent fruit whose quality is not affected by only BER and cracks but with also mechanical damages during transportation and handling. This study exploits the advantages of LAB color space to perform tomato defect detection. 500 images of tomatoes with different degree of defect were randomly selected and were converted from RGB to LAB. The intensity values of L, A, and B space were then extracted from each pixel points for each image and were labeled as either defect or healthy pixels. Let the extracted color space features be denoted by LM which was a huge matrix of I_s *by* 4, for the 500 images, 3 color spaces and the pixel label as 1 for healthy and −1 for defected, where I_s is the total number of pixels in all the images ($1280 * 720 * 500$). LM was split into training and validation datasets of 0.7 and 0.3 of the total observations respectively. Each observation of the training dataset can be presented by (LMt_r,Xt_r). Where, $LMt \subset LM$, Xt_r is the label corresponding to LMt_r, and $r \in [1, (0.7 * I_s)]$ The training dataset was used to train a radial basis function (RBF-SVM) classifier. The modeled classifier was then validated by the $0.3 * I_s$ observations denoted by (LMs_e,Xs_e). Where, $e \in [1, (0.3 * I_s)]$, $LMs \subset LM$, Xs_e is the label corresponding to LMs_e. The validation results obtained was denoted by p_e for each LMs_e. The value of each e in Xs_e was compared to p_e, the performance of the defect detection model was evaluated according to Eq. (2).

$$\frac{num(Xs_e == p_e)}{num(Xs_e)} \; k \in [1, (0.3 * I_s)] \tag{2}$$

where $num(Xs_e = = p_e)$ is the number of p_e that equals Xs_e.

2.4. Feature extraction

2.4.1. Color features

Color features are also referred to as statistical features (1st order spatial statistics measure). In this study, LAB color space was used due to its ability of limited variance due to sensor sensitivity (Shafiee et al., 2014). LAB color space is a 3-axis color system with absolute and predefined range for the L, A, and B dimensions. Where L represents the brightness (the darkest black at L = 0, and the brightest white at L = 100), A and B represent the color channels. A represents red and green opponent colors along the A axis at positive and negative values, respectively. B represents yellow and blue opponent colors along the B axis at positive and negative values, respectively. However, at A = 0 and B = 0 represents true neutral gray values (Margulis, 2005). In LAB color space, all colors in the spectrum are considered, as well as colors outside the human perception (Hashim et al., 2012; Hu et al., 2016). From each space, three color features were extracted (mean, standard deviation, and range). Thus, a total of nine color features were extracted in each image. These color features depend only on the individual pixel values but do not account for the relative relations of the gray values (Moallem et al., 2017). Fig. 5 shows the conversion of the original RGB image into LAB color space.

2.4.2. Texture features

Texture features are also referred to as a 2nd order measure. These features present the gray values of pixels in pairs. Thus, they capture the spatial dependence of gray values. In this study, Haralick textural features were computed from Gray-Level Cooccurrence Matrices (GLCM) (Haralick and Shanmugam, 1973; Moallem et al., 2013). A 2D GLCM matrix presented each image, and the textual features are the average of this matrix using neighborhood of distance $d = 1$ towards the directions 0^0, 45^0, 90^0, and 135^0 this is because defects have no specific direction. The extracted features were the contrast, correlation, energy, homogeneity and entropy.

2.4.3. Shape features

Shape regularity is often used as a quality measure in marketing. Tomatoes with regular shapes are often considered as of better quality. The tomato shape asymmetrical value was computed as a measure of shape regularity. A binary image of the tomato was obtained by image binarization (Otsu, 1979). Then the edges were extracted by the Sobel operator. The regularity measure (ξ) was then extracted according to Eq. (3). Where, $d_r(t)$ and $d_l(t)$ are the horizontal distances between the boundary point and the longitudinal line through the image

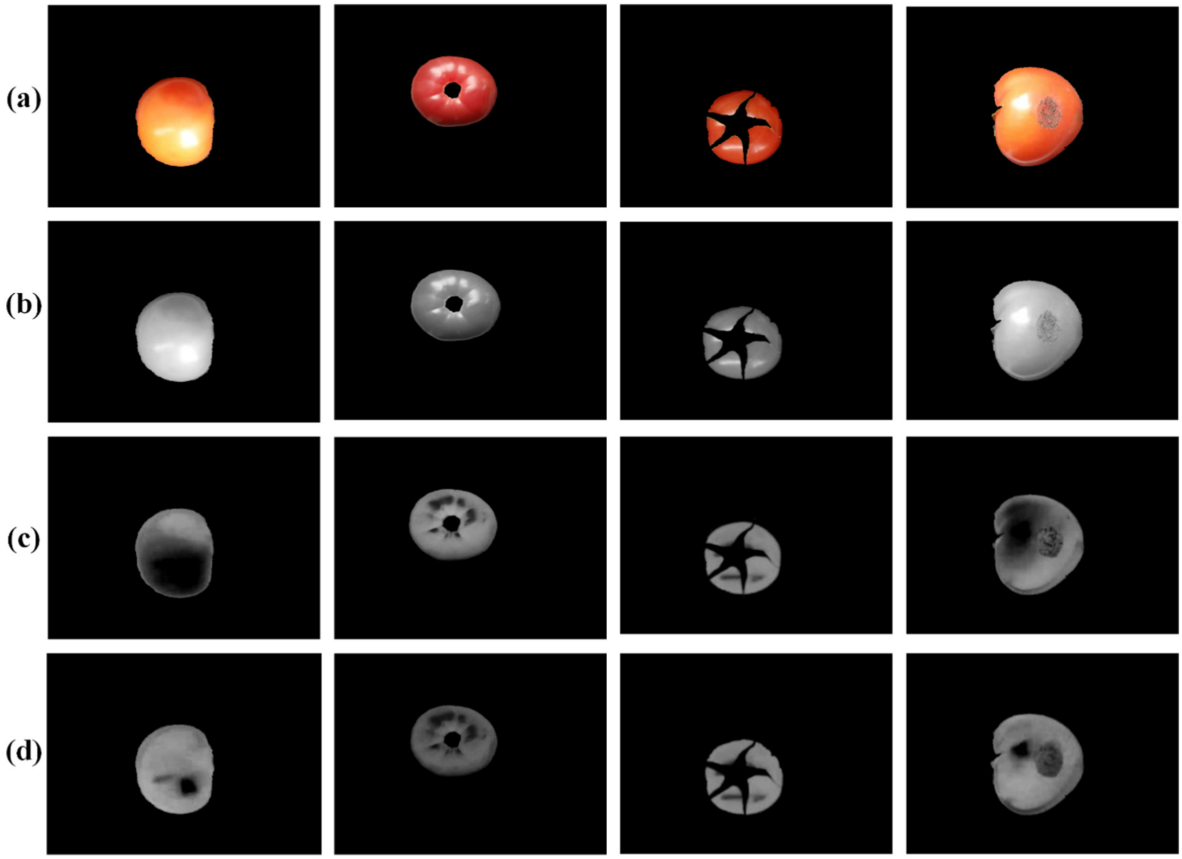

Fig. 5. Conversion of the color image to LAB color space, (a) RGB image, (b) L-space of LAB, (c) A-space of LAB, and (d) B-space of LAB.

centroid on the right-hand side and left-hand side respectively.

$$\xi = \left(\frac{\sum_1^t |d_r(t) - d_l(t)|}{\sum_1^t |d_r(t) + d_l(t)|} \right) \tag{3}$$

2.5. Recognition models

The captured tomato images were manually labeled by a human expert into four groups depending on defect, healthy, and ripeness (red color intensity): healthy and defected (cat 1). Secondly, 1st grade, 2nd grade, and rejected (cat 2). Thirdly, healthy deep red, healthy light red, and defected (cat 3). Lastly, 1st grade deep red, 1st grade light red, 2nd grade deep red, 2nd grade light red and rejected (cat 4) as shown in Table 1. A classification model was then developed, and the obtained results were compared to those of human expert. A total of fifteen features were extracted from each image. Based on the quality grading, a total of four models were developed for each recognition model explored. The recognition models were linear-SVM, quadratic-SVM, cubic-SVM, and radial basis function (RBF-SVM), ANN, decision tree, and random forest. These models were trained by a 10-fold cross-validation-based parameter search on the training dataset after which they were further evaluated on a testing dataset. A comparison to the manual labeling of the testing dataset was presented in terms of recognition accuracy.

Table 1
The dataset for all the grading categories explored.

Grading categories	Healthy			Defected
cat 1	1200			800
cat 2	1st grade	950		600
	2nd grade	450		
cat 3	Deep red	800		800
	Light red	400		
cat 4	1st grade	Deep red	600	600
		Light red	350	
	2nd grade	Deep red	250	
		Light red	200	

2.5.1. The SVM recognition models

SVM is a widely used regression technique and a statistical classifier based on a supervised learning algorithm (Kim and Choi, 2014). Generally, supervised learning algorithms vectors are input nonlinearly into a high-dimensional feature space. The SVM algorithm determines the maximum margin in the high-dimensional feature space by applying the principle of construction risk minimization to classify the tomatoes into required categories. This study explored the linear, quadratic, cubic, and radial basis kernel functions. The choice of kernel function affects the overall performance of an SVM classifier in terms of efficiency and accuracy. Eqs. (4) to (6) presents the basic kernel functions, i.e., linear, polynomial and radial basis kernel functions. For more review on SVM, please refer to the study by (Chang and Lin, 2011).

$$K(x_i, x_j) = x_i^T x_j \tag{4}$$

$$K(x_i, x_j) = \left(\gamma x_i^T x_j + 1\right)^d, \gamma > 0 \tag{5}$$

$$K(x_i, x_j) = e^{-\gamma \|x_i - x_j\|^2}, \gamma > 0 \tag{6}$$

Table 2
Calyx extraction algorithm performance on a testing dataset.

Dataset	Accuracy	RMSE
Healthy	0.9767	8
Defected	0.9263	59
Average	0.9515	33.5

2.5.2. The ANN recognition models

The ANN applied in this study was a one-hidden-layer feed-forward network trained by back propagation. The general equation of the ANN model is given in Eq. (7). Where, q is the output, p_i is the extracted features (in this study $=1, 2 \ldots 15$), w_i is the mass of the i^{th} input, b is the bias, and f is the transfer function.

$$q = f\left(\sum_{i=1}^{15} w_i p_i + b\right) \tag{7}$$

The developed ANN models had three layers; input layer, hidden layer, and the output layer. The input layer had fifteen inputs corresponding to the extracted features. The number of neurons in the hidden layer was set to 10 after an exhaustive search with an increasing number of neurons to establish a minimum percent error during the validation phase. A hyperbolic tangent sigmoid transfer function was used in the hidden layer, while a linear transfer function was used in the output layer.

The image acquisition system captured a total of 2000 images. As presented in Table 1. Above, in each grading category, 70% of the dataset was used as a model training dataset while the remaining was used as the testing dataset. The performance of each model for each grading category was then presented in terms of accuracy in comparison to manual labeling.

3. Results and discussion

3.1. Calyx and stalk scar detection analysis

The CS extraction algorithm was applied to 500 images with calyx and stalk scar. The test achieved an average accuracy of 0.9515 and RMSE of 33.5 tomato images on the dataset, as shown in Table 2. However, on separate datasets of healthy and defected, the defected achieved a lower accuracy as shown in Table 2, this was mainly due to defect and CS having almost similar color intensities at different and varying ambient light levels.

Different calyx detection techniques already exist from several studies on fruit and vegetables sorting such as the used of K-means clustering on Cb component in YCbCr color space by Moallem et al. (2017) in apple grading. Image object segmentation and thresholding by Arakeri (2016) in tomato sorting and grading. However, to improve on the calyx detection accuracy and reduce the computational time for real time online system this study applied the methodology presented by Liming and Yanchao (2010) in the strawberry grading system by establishing the average g-r thresholding value and applied it to all the images.

3.2. Defect detection analysis

Defect detection was performed after extraction of CS to prevent a mismatch between CS and a defect. This study selected the RBF kernel because of its ability to always adapts well by varying its scaling factor in a large range of problems (Han et al., 2012). The results show that the developed defect model could identify defected pixels with an accuracy of 0.989 on the validation dataset. Fig. 6 shows the identification of defected pixel regions using the introduced methodology.

As already mentioned, defects can often result from several factors such as mechanical bruising, black BER, freezing injury, sunscald, and decay. Several studies have already been presented in the detection of these defects. Dhanabal and Samanta (2013) presented a color image

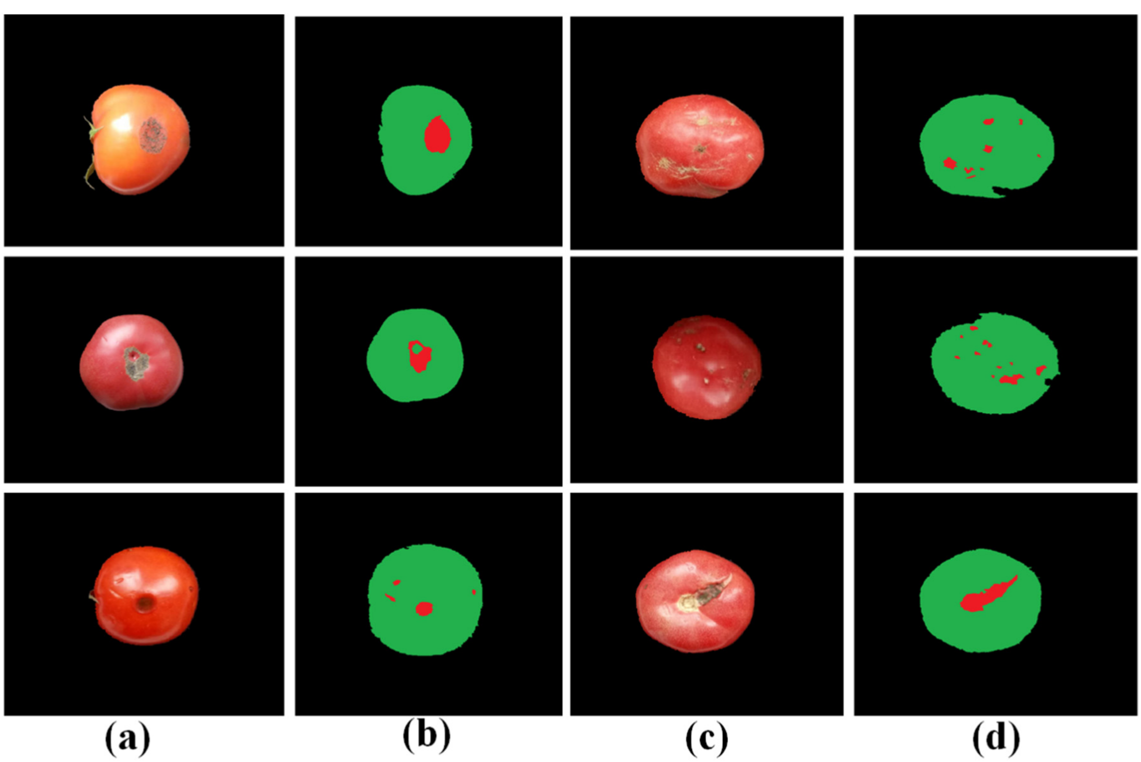

Fig. 6. Defect detection process on a tomato (a) and (c), original tomato image with defects (b) and (d) detected defect and healthy regions on the tomatoes (green is indicating healthy pixel while red indicating defected pixels).

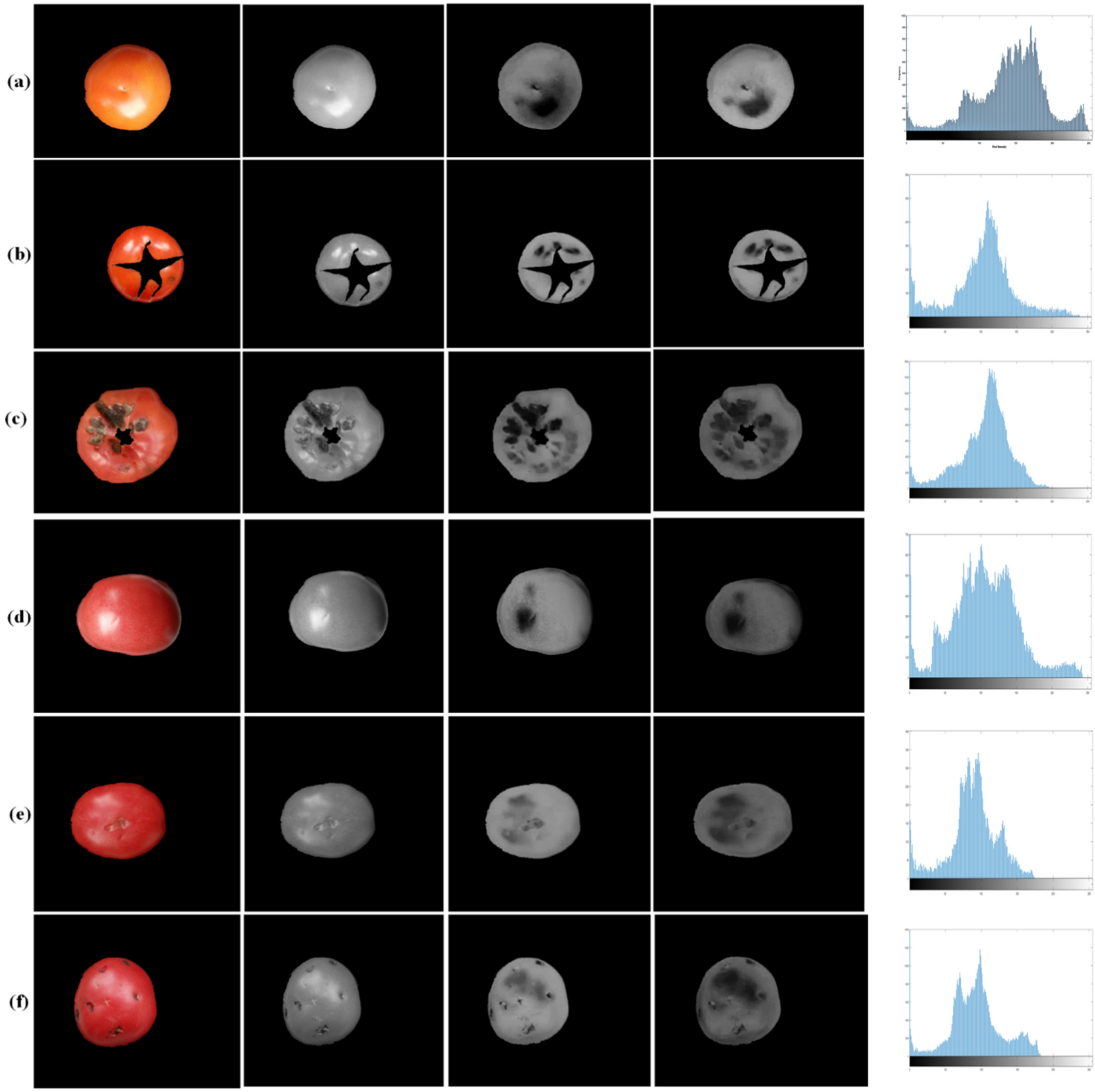

Fig. 7. Different tomato quality with their respective LAB color space and histogram (a) healthy light red (b) healthy with calyx (c) rejected (d) healthy deep red (e) second grade deep red (f) rejected.

threshold method to discriminate unripe, ripe and spoiled tomatoes. Lee et al. (2008) developed near-infrared imaging system in the grading of date fruits at an overall accuracy of 95.0%, despite the high accuracy of high-quality images like the hyperspectral, multispectral and near-infrared imaging the costs involved are always much higher in the setup of such systems. Never the less this introduced system despite image quality is sensitive to ambient light conditions still achieved a high accuracy due to controlled lighting.

3.3. Grading categories analysis

This study introduces an automated technique for tomato sorting. A machine vision system was designed to extract tomato image features based on color, texture, and shape parameters. A detailed image processing technique for real time inline tomato evaluation was introduced. Fig. 7 presents the image analysis of different gradings of tomatoes used in this proposed grading system together with their corresponding histograms. It was established that a healthy tomato (Fig. 8) had significantly higher pixel values than defected tomatoes.

Based on the developed recognition models, Table 3 presents the recognition accuracy for all the explored models. It can be observed that the RBF-SVM outperformed all the models based on the accuracy in recognition results on the testing dataset. In marketing, tomatoes are sorted based on different categories.

This study presents four grading categories, and the performance of each classification is evaluated. It was also observed that as the

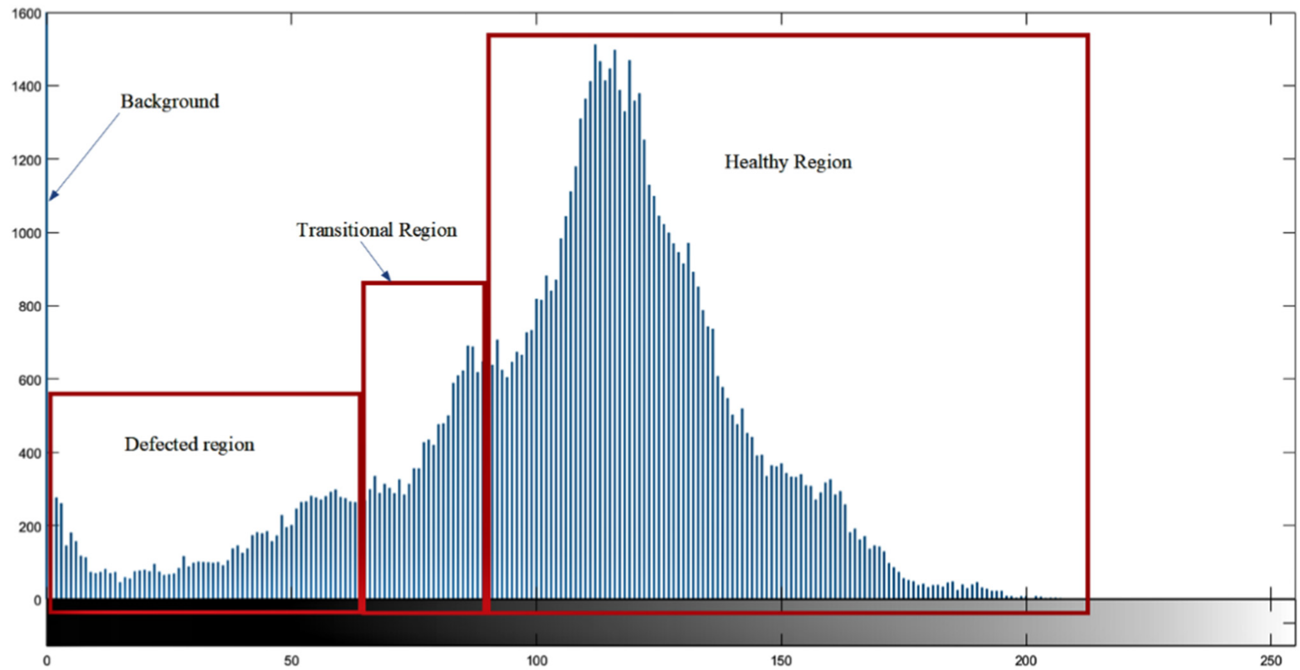

Fig. 8. Pixel intensity differences distinguishing the background, defected, transition and heathy tomato regions.

recognition accuracy decreases with the increase in the grading categories as presented in Table 3. However, the overall accuracy results of the proposed system are sufficiently acceptable in practical applications.

3.4. Two grades category (cat 1) grading

It is observed that the RBF-SVM outperforms all the other models at an accuracy of 0.9709. A confusion matrix in Table 4 shows the statistical measures of the performance of the RBF-SVM cat 1 model using the criteria accuracy = (TP + TN)/ (TP + TN + FP + FN), specificity = TN/(TN + FP), precision = TP/(TP + FP) and sensitivity = TP/(TP + FN); where TP is True Positive, TN is True Negative, FP is False Positive and FN is False Negative. The result of the classification achieved a specificity of 0.9613, precision of 0.9742, and sensitivity of 0.9775 on the testing dataset.

3.5. Three grades category (cat 2) grading

The three quality categories include the 1st grade, 2nd grade and rejects based on the degree of defects, 1st grade was defects free, 2nd grade had a lower degree of defects while reject had a higher degree of the defect according to the observation by a tomato grading professional. From Table 3, it can be observed that RBF-SVM again outperformed all the explored models to have the highest recognition accuracy of 0.9542. The statistical performance of the RBF-SVM model in grading in cat 2 is given in Table 5.

Table 3
Performance of all the explored models for each category of tomato grading.

Grading categories	SVM models				ANN	Random forest
	Linear	Quadratic	Cubic	RBF		
cat 1	0.9467	0.9624	0.8961	0.9709	0.9583	0.9412
cat 2	0.9301	0.9267	0.9278	0.9542	0.9421	0.9395
cat 3	0.9126	0.9035	0.9126	0.9691	0.9486	0.9255
cat 4	0.9278	0.9108	0.8835	0.9385	0.9299	0.9107

Table 4
Confusion matrix for recognition in cat 1 grading.

Grading system labeling	Manual labeling		Total
	Healthy	Defected	
Healthy	1173	31	1204
Defected	27	769	796

3.6. Three grades category (cat 3) grading

This grading category was similar to cat 1 grading but with the addition of color grading of the healthy tomatoes. Color is an essential factor in grading in terms of ripeness (market readiness) in supply chain management (Jahns et al., 2001). The RBF-SVM achieved the highest accuracy at 0.9691. The analytical performance of the RBF-SVM model in grading in cat 3 is given in Table 6.

3.7. Five grades category (cat 4) grading

This grading category was similar to cat 2 with a further color feature to sort the 1st grade and 2nd grades into deep red and light red grades. It can be observed from Table 3 and Table 7 that RBF-SVM have the highest accuracy of 0.9385. The statistical performance of the RBF-SVM model in grading in cat 3 is given in Table 7.

3.8. Extracted features analysis

This study presented an analysis of all the extracted feature variables to determine the performance of each feature variable as predictors in

Table 5
Confusion matrix for recognition in cat 2 grading.

Grading system labeling	Manual labeling			Total
	1st grade	2nd grade	Rejects	
1st grade	918	19	6	946
2nd grade	25	424	28	465
rejects	7	5	566	589

Table 6
Confusion matrix for recognition in cat 3 grading.

Grading system labeling	Manual labeling			Total
	Healthy (deep red)	Healthy (light red)	Defected	
Healthy (deep red)	788	39	1	828
Healthy (light red)	12	356	5	373
Defected	0	5	794	799

each grading category. RBF-SVM models were developed based on each feature variables and a combination of all the variables and were tested on the validation dataset. The results were then presented in terms of model accuracy. The extracted features were nine color features, five texture features, and one shape feature as presented in the Materials and methods section. It was established that all feature variables combination improved the overall performance of the recognition model, as shown in Fig. 8. It can also be observed that shape feature was the poorest predictor followed by color feature then texture feature. Similarly, it was observed that the accuracy of the different models decreased as the number of grading categories increased, as shown in Fig. 9.

4. Conclusion

This study proposes a tomato defect detection system on image color, texture, and shape features. A relation of the tomato image LAB color space to defect was developed. The results obtained suggest that the proposed machine vision system can be used to detect defects in Cherry and Heirloom tomatoes. However, this system needs to be validated on other varieties of tomatoes, despite these shortcomings, the proposed technique with acceptable results achieved the objectives of this research study. It is of great importance to detect defects in tomatoes during post-harvest processing for quality inspection, marketing, and packaging. Thus, this proposed system can be applied as an inline grading and sorting system in tomato post harvesting. This introduced system can also be integrated with other grading criteria such as weight, volume, and shape estimation systems in post-harvest management of tomatoes.

Table 7
Confusion matrix for recognition in cat 4 grading.

Grading system labeling	Manual labeling					Total
	1st grade (DR)	1st grade (LR)	2nd grade (DR)	2nd grade (LR)	Rejects	
1st grade (DR)	572	8	11	4	2	596
1st grade (LR)	9	323	3	9	5	347
2nd grade (DR)	11	6	229	3	7	259
2nd grade (LR)	3	7	4	178	11	204
Rejects	5	6	3	6	575	594

Acknowledgements

We thank the editor and the reviewers for assisting in improving the manuscript and acknowledge Fundamental Research Funds for the Central Universities, China (KYGX201701) for funding the research.

References

Al Ohali, Y., 2011. Computer vision based date fruit grading system: design and implementation. J. King Saud Univ. –Comput. Inf. Sci. 23 (1), 29–36.
Arakeri, M.P., 2016. Computer vision based fruit grading system for quality evaluation of tomato in agriculture industry. Procedia Comput. Sci. 79, 426–433.
Arjenaki, O.O., Moghaddam, P.A., Motlagh, A.M., 2013. Online tomato sorting based on shape, maturity, size, and surface defects using machine vision. Turk. J. Agric. For. 37 (1), 62–68.
Blasco, J., Aleixos, N., Molto, E., 2007. Computer vision detection of peel defects in citrus by means of a region oriented segmentation algorithm. J. Food Eng. 81 (3), 535–543.
Chang, C.-C., Lin, C.-J., 2011. LIBSVM: a library for support vector machines. ACM Trans. Intell. Syst. Technol. (TIST) 2 (3), 27.
Chen, Y.-R., Chao, K., Kim, M.S., 2002. Machine vision technology for agricultural applications. Comput. Electron. Agric. 36 (2–3), 173–191.
Clement, Novas, Gázquez, J.A., Manzano-Agugliaro, F., 2012. High speed intelligent classifier of tomatoes by colour, size and weight. Span. J. Agric. Res. 10 (2), 314–325.
Clement, Novas, José-Antonio, G., Francisco, M.-A., 2013. An active contour computer algorithm for the classification of cucumbers. Comput. Electron. Agric. 92, 75–81. https://doi.org/10.1016/j.compag.2013.01.006.
Dhanabal, T., Samanta, D., 2013. Computerized spoiled tomato detection. Int. J. Res. Eng. Technol. 2, 38–41.
Esguerra, E., Rolle, R., & S, R. (2018). Post-harvest Management of Tomato for Quality and Safety Assurance (TCP/RAS/3502), 1–20. Retrieved from http://www.fao.org/3/I8236EN/i8236en.pdf
EU, 2011. Fruit and Vegetables: Marketing Standards. Retrieved from. https://ec.europa.eu/agriculture/fruit-and-vegetables/marketing-standards_en.
FAO. (2008). Standard for Tomatoes 293, 1–5. Retrieved from http://www.fao.org/fao-who-codexalimentarius/shproxy/it/?lnk=1&url=https%253A%252F%252Fworkspace.fao.org%252Fsites%252Fcodex%252FStandards%252FCODEX%2BSTAN%2B293-2008%252FCXS_293e.pdf
FAOSTAT, 2017. Tomatoes, Production Quantity (Tons) - for All Countries. Retrieved from. http://www.factfish.com/statistic/tomatoes%2C%20production%20quantity.
Gould, W.A., 1975. Mass Sorting of Mechanically Harvested Tomatoes.
Han, S., Qubo, C., Meng, H., 2012. Parameter Selection in SVM With RBF Kernel Function. Paper Presented at the World Automation Congress. p. 2012.
Haralick, R.M., Shanmugam, K., 1973. Textural features for image classification. IEEE Trans. Syst. (6), 610–621 man, and cybernetics.

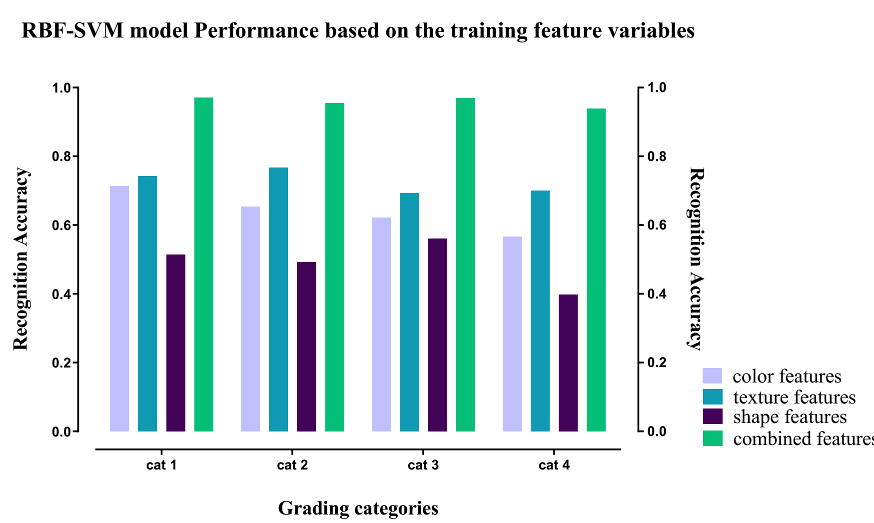

Fig. 9. A comparison of the effectiveness of the extracted feature variables in tomato grading.

Hashim, N., Janius, R.B., Baranyai, L., Rahman, R.A., Osman, A., Zude, M., 2012. Kinetic model for colour changes in bananas during the appearance of chilling injury symptoms. Food Bioprocess Technol. 5 (8), 2952–2963.

Hu, M.H., Dong, Q.L., Liu, B.L., Pan, L.Q., Walshaw, J., 2016. Image segmentation of bananas in a crate using a multiple threshold method. J. Food Process Eng. 39 (5), 427–432.

Jahns, G., Nielsen, H.M., Paul, W., 2001. Measuring image analysis attributes and modelling fuzzy consumer aspects for tomato quality grading. Comput. Electron. Agric. 31 (1), 17–29. https://doi.org/10.1016/S0168-1699(00)00171-X.

Jarimopas, B., Jaisin, N., 2008. An experimental machine vision system for sorting sweet tamarind. J. Food Eng. 89 (3), 291–297.

Karlsson, P. (2016). Is Manual Harvest Really Better Than Mechanical Harvest? Retrieved from https://www.bkwine.com/features/winemaking-viticulture/raw-truth-manual-mechanical-harvest/

Kim, S., Choi, J., 2014. An SVM-based high-quality article classifier for systematic reviews. J. Biomed. Inform. 47, 153–159.

Lee, D.-J., Schoenberger, R., Archibald, J., McCollum, S., 2008. Development of a machine vision system for automatic date grading using digital reflective near-infrared imaging. J. Food Eng. 86 (3), 388–398.

Liming, X., Yanchao, Z., 2010. Automated strawberry grading system based on image processing. Comput. Electron. Agric. 71, S32–S39.

López-García, F., Andreu-García, G., Blasco, J., Aleixos, N., Valiente, J.-M., 2010. Automatic detection of skin defects in citrus fruits using a multivariate image analysis approach. Comput. Electron. Agric. 71 (2), 189–197.

Margulis, D., 2005. Photoshop LAB Color: The Canyon Conundrum and Other Adventures in the Most Powerful Colorspace. Peachpit Press.

Moallem, Razmjooy, 2012. Optimal threshold computing in automatic image thresholding using adaptive particle swarm optimization. J. Appl. Res. Technol. 10 (5), 703–712.

Moallem, P., Razmjooy, N., Ashourian, M., 2013. Computer vision-based potato defect detection using neural networks and support vector machine. Int. J. Robot. Autom. 28 (2), 137–145.

Moallem, P., Serajoddin, A., Pourghassem, H., 2017. Computer vision-based apple grading for golden delicious apples based on surface features. Inf. Process. Agric. 4 (1), 33–40.

Moltó, E., Blasco, J., Gómez-Sanchís, J., 2010. Analysis of hyperspectral images of citrus fruits. Hyperspectral Imaging for Food Quality Analysis and Control. Elsevier, pp. 321–348.

Naik, S., & Patel, B. (2014). CIELab based color feature extraction for maturity level grading of Mango (*Mangifera indica* L.). National Journal of System and Information Technology, 0974–3308.

Naik, S., Patel, B., & Pandey, R. (2015). Shape, size and maturity features extraction with fuzzy classifier for non-destructive mango (*Mangifera indica* L., cv. Kesar) grading. Paper Presented at the 2015 IEEE Technological Innovation in ICT for Agriculture and Rural Development (TIAR).

Nandi, C., Tudu, B., Koley, C., 2014. Machine vision based techniques for automatic mango fruit sorting and grading based on maturity level and size. Sensing Technology: Current Status and Future Trends II. Springer, pp. 27–46.

Otsu, N., 1979. A threshold selection method from gray-level histograms. IEEE Trans. Syst. Man Cybern. 9 (1), 62–66.

Polder, G., van der Heijden, G., 2010. Measuring ripening of tomatoes using imaging spectrometry. Hyperspectral Imaging for Food Quality Analysis and Control. Elsevier, pp. 369–402.

Rokunuzzaman, M., Jayasuriya, H., 2013. Development of a low cost machine vision system for sorting of tomatoes. Agric. Eng. Int. CIGR J. 15 (1).

Sarkar, N., Wolfe, R., 1985. Computer vision based system for quality separation of fresh market tomatoes. Trans. ASAE 28 (5), 1714–1718.

Shafiee, S., Minaei, S., Moghaddam-Charkari, N., Barzegar, M., 2014. Honey characterization using computer vision system and artificial neural networks. Food Chem. 159, 143–150.

Unay, D., Gosselin, B., Kleynen, O., Leemans, V., Destain, M.-F., Debeir, O., 2011. Automatic grading of bi-colored apples by multispectral machine vision. Comput. Electron. Agric. 75 (1), 204–212.